Thermal Stresses due to Electrical discharge machining on AISI4340

Department of Mechanical Engineering, Bundelkhand Institute of Engineering and Technology Jhansi, India

Shruti Saxena
Email id : shruti11mec@gmail.com

Abstract

A finite element model has been developed to estimate the thermal stresses due to Gaussian distributed heat flux of a spark during EDM. The developed model first calculates the temperature distribution in the work piece material using ANSYS software. The results of the analysis show high temperature gradient zones and the regions of large stresses where, sometimes, they exceed the material yield strength. Results from thermal concern thermal stresses be compared with the experimental values. And find out the effect on the creater surface.

1. INTRODUCTION

Electrical Discharge Machining (EDM) is a controlled metal-removal process that is used to remove metal by means of electric spark erosion. In this process an electric spark is used as the cutting tool to cut (erode) the workpiece to produce the finished part to the desired shape. The metal-removal process is performed by applying a pulsating (ON/OFF) electrical charge of high-frequency current through the electrode to the workpiece. This removes (erodes) very tiny pieces of metal from the workpiece at a controlled rate. The material removal is takes place due to localized heating and then vaporization of material during machining. When an electrostatic field of sufficient strength is established then electrons accerate towards the anode. Ultimately a series of narrow columns of ionized dielectric fluid molecules is established, connecting two electrodes causing an avalanche of electrons since the conductivity of the ionized column is very large which is normally seen as a spark. As a result of this spark a compression shock waves is generated and a very high temperature is developed on the electrodes.

Various aspects of EDM process have been studied in detail like types of EDM machines Wire cut/Die-sinking), tooling, control circuits, process performance under chosen conditions, on-line machine control, etc., [1-3]. In the present context, studies on the development of analytical process models of die-sinking EDM process are particularly relevant.

2. LITERATURE REVIEW

Since the early seventies, researches worldwide attempted to thermal model of electrical discharge machining and serach out the thermal stresses in the material AISI 4340.

Vinod Yadav et al. (2002) proposed that the high temperature gradients generated at the gap during EDM result in large localized thermal stresses in a small heat-affected zone leading to micro-cracks, decrease in strength and fatigue life and possibly catastrophic failure.

J. Marafona et al. (2005) has presented the amount of heat dissipated varies with the thermal–physical properties of the conductor; as a result, the maximum temperature reached is different.

Nizar Ben Salah et al. (2006) presented numerical results concerning the temperature distribution due to electric discharge machining process. From these thermal results, the material removal rate and the total roughness were deduced and compared with experimental observations.

Philip Allen et al, (2007) has presented thermal stresses is analyzed using a thermo-numerical model, which simulates a single spark discharge process.

H.K. Kansal et al**,** (2008) proposed the developed model first calculates the temperature distribution in the workpiece material using ANSYS software and then material removal rate (MRR) is estimated from the temperature profiles.

3. THERMAL MODELLING

Due to the random and complex nature of EDM, the following assumptions are made to make the problem mathematically tractable.

ASSUMPTIONS

1. The model is developed for a single spark in view of the fact that machining by EDM is a succession of elementary discharges.
2. The material properties of the workpiece and tool are temperature dependent.
3. Inertia and body force effects are negligible during stress development.
4. The domain is considered as axisymmetric.
5. Work piece and tool materials are homogeneous and isotropic in nature.
6. Heat flux is assumed to be Gaussian distributed [17]. The zone of influence of the spark is assumed to be axi-symmetric in nature.

GOVERNING EQUATIONS

3.1 Equilibrium equations

These equations are derived from the force equilibrium of a point.

$$\frac{\partial \sigma_{rr}}{\partial r} + \frac{\partial \sigma_{rz}}{\partial z} + \frac{\sigma_{\theta\theta} + \sigma_{rr}}{r} = 0 \quad (1)$$

$$\frac{\partial \sigma_{rr}}{\partial r} + \frac{\partial \sigma_{zz}}{\partial z} + \frac{\sigma_{rz}}{r} = 0 \quad (2)$$

Where, σ_{rr}, σ_{zz} and $\sigma_{\theta\theta}$ are normal stresses and σ_{rz} is shear stress. Here the body and initial forces are neglected.[3]

3.2 Strain-displacement relations

$$\varepsilon_{rr} = \frac{\partial u}{\partial r}, \quad \varepsilon_{\theta\theta} = \frac{u}{r}, \quad \varepsilon_{zz} = \frac{\partial w}{\partial z}, \quad \varepsilon_{rz} = \frac{\partial u}{\partial z} + \frac{\partial w}{\partial r}$$

Here ε_{rr}, $\varepsilon_{\theta\theta}$ and ε_{zz} are normal strains, ε_{rz} is shear strain, and *u* and *W* are displacements.[3]

3.3 Constitutive relations

The stress–strain relationship due to temperature rise ΔT can be written as:

$$\{\sigma\} = [D]\{\varepsilon\} - \{m\} \tag{3}$$

where [*D*] is the elasticity matrix, {σ} is the stress vector and { ε} is the strain vector. The expressions for {σ}, { ε}, {*m*} and [*D*] are as follows:

$$\{\sigma\}^T = \{\sigma_{rr}, \sigma_{\theta\theta}, \sigma_{zz}, \sigma_{rz}\} \tag{4}$$

$$\{\varepsilon\}^T = \{\varepsilon_{rr}, \varepsilon_{\theta\theta}, \varepsilon_{zz}, \varepsilon_{rz}\} \tag{5}$$

$$\{m\} = \begin{Bmatrix} 1 \\ 1 \\ 1 \\ 0 \end{Bmatrix} \frac{E\alpha_1 \Delta T}{1-2v} \tag{6}$$

$$[D] = \frac{E}{(1+v)(1-2v)} \begin{bmatrix} 1-v & v & v & 0 \\ v & 1-v & v & 0 \\ v & v & 1-v & 0 \\ 0 & 0 & 0 & \frac{1-2v}{2} \end{bmatrix} \tag{7}$$

Here, *E* is young's modulus, v is Poisson's ratio and α_1 is coefficient of thermal expansion.[3]

3.4 Boundary conditions

Eqs. (1, 2) are a set of elliptic equations in unknown displacements u and w, thus

requiring boundary conditions along the boundary surface of the domain under consideration. Displacements along and across surface AD (Fig. 1) are assumed zero.

$u=0$ and $w = 0$ on AD

Since AB is an axis of symmetry the normal component of displacement vector and shear component of traction vector are zero along the boundary. Thus,

$u=0$ and $t_z = 0$ on AB

Furthermore, since BC is a free surface, both the traction components are zero on this boundary. Finally, the boundary CD is considered sufficiently far away from the heat source so as to be stress free. Thus, the boundary conditions on BC and CD are

$t_r = 0$ and $t_z = 0$ on BC and CD

The traction components t_r and t_z are related to the components of the stress tensor by the following relation:

$$t_i = \sigma_{ij} n_j$$

where, n_j are the components of the unit outward normal vector.

where, n_j are the components of the unit outward normal vector.

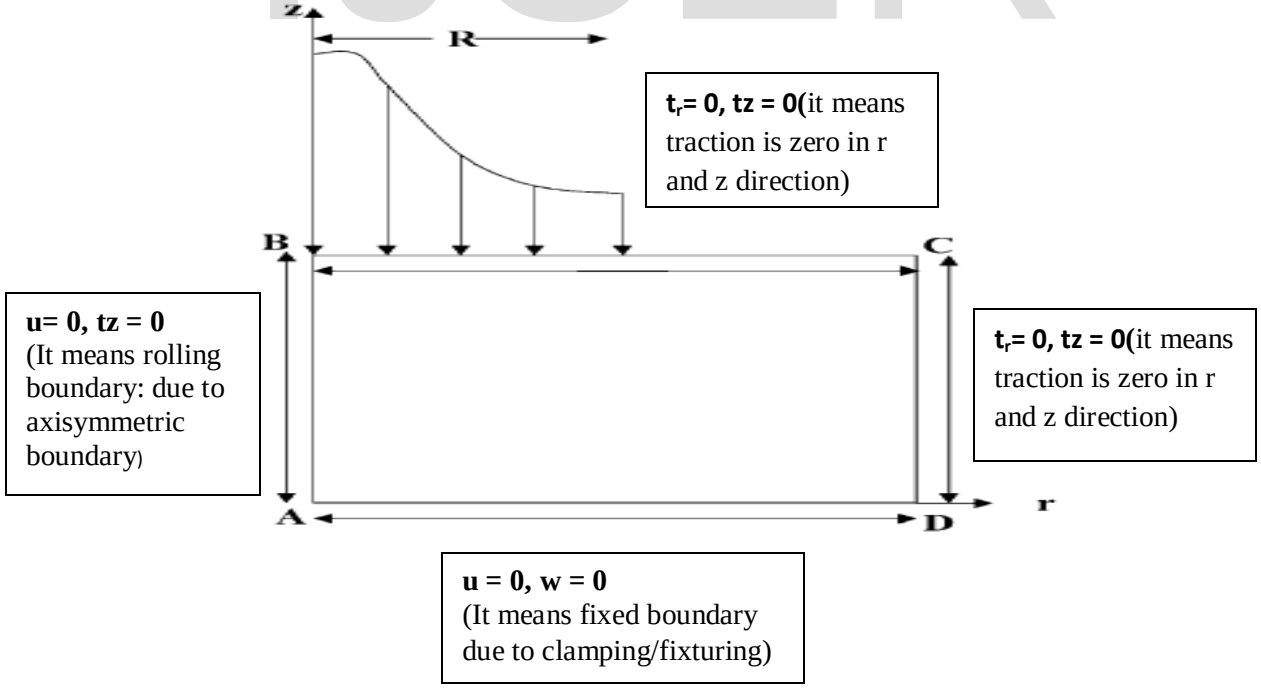

- u,w : nodal displacements in r and z direction respectively.
- t_r and t_z : traction component of force in r and z direction respectively.

4. INDUCED THERMAL RESIDUAL STRESSES

Once the temperature distribution was obtained, and the removed material then the thermal residual stresses can be determined. The Figs. 5.5 and 5.6 are finite element plots that illustrate the thermal residual stress distributions directly after the heat flux. Thermal stress in the r-direction as shown in Figs. 5.5 indicates that compressive thermal stresses surround the created crater at this point in time. The largest compressive stress in the r-direction is -190MPa and is on the edge of the crater where as the minimum compressive stress is -3230MPa moving away from the crater both r-dire -ction and z-direction, the compressive stresses become less and less. This can easily be explained, as the material heats up during the heat flux, it is not able to instantaneously expand causing compressive thermal stresses in the heated zone.

Now the transient temperature distribution figure shows below at 500 microsec.

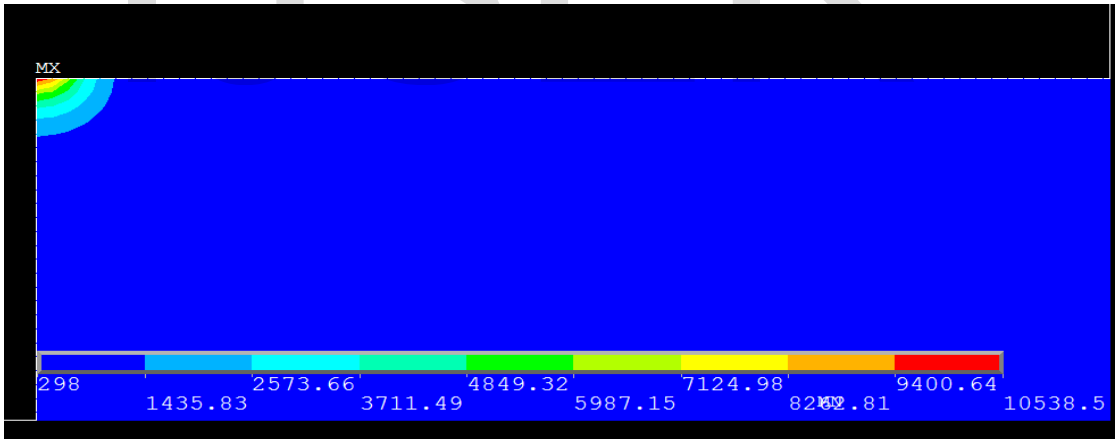

Fig.1 Temperature distribution obtained at the end of spark after 500 µs.

When the temperature distribution can be find after 500 µs, the highest temperature of the material is 10537K where the melting point of the AISI4340 is 1427K. at this high temperature the material begins to evaporate the material. With the help of ANSYS, the element death procedure have done and the material removed at 500 µs can be easily found.

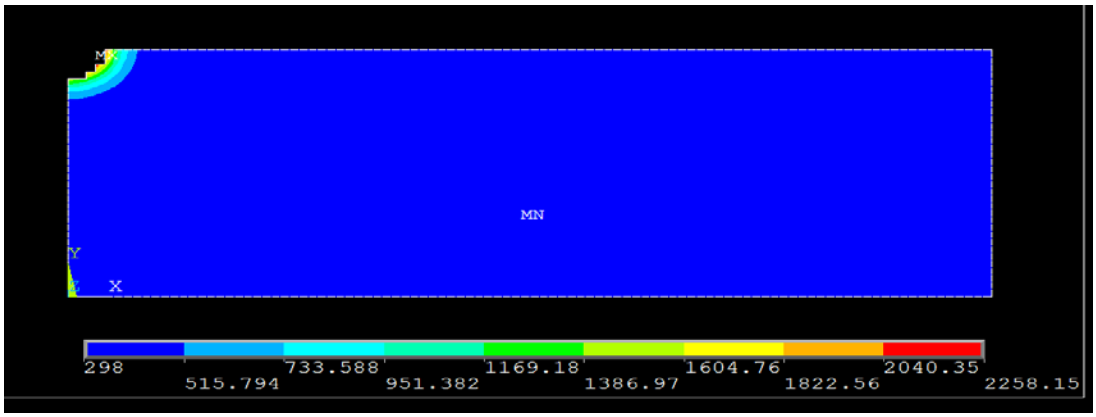

Fig. 2 Material removal after 500µs

Fig. 3 and 4 shows the thermal residual stresses. After the cooling period is complete, the once compressive stresses around the crater after heating have changed to tensile stresses. As the depth increases below the crater, the stresses transition into compressive residual stresses; these compressive stresses bring the equilibrium to the system.

As the cooling duration increases, the compressive stresses around the crater gradually transition to a combination of both compressive and tensile stresses. The highest tensile stresses are seen at the crater boundary. The transition stresses in the workpiece are greatest when the transition initially occurs. As the cooling-time progresses they reduce; these are the residual stresses left in the workpiece from the single-spark heat-flux. During the cooling period, the compressive stresses in the z-direction gradually decrease as shown in Fig.4. This figure illustrates how the compressive stresses in the workpiece change with the workpiece depth.

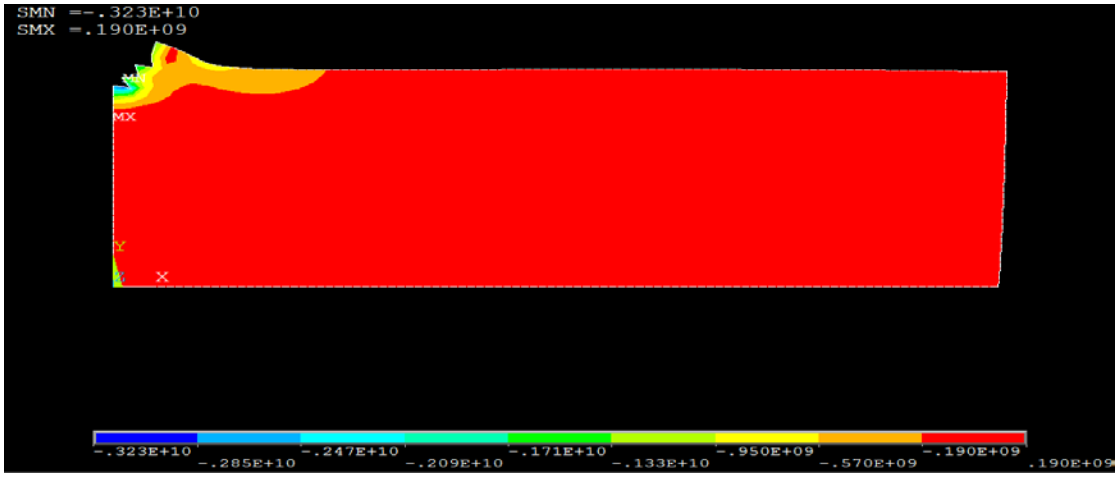

Fig.3 Residual Thermal stress in workpiece AISI 4340 in r-direction

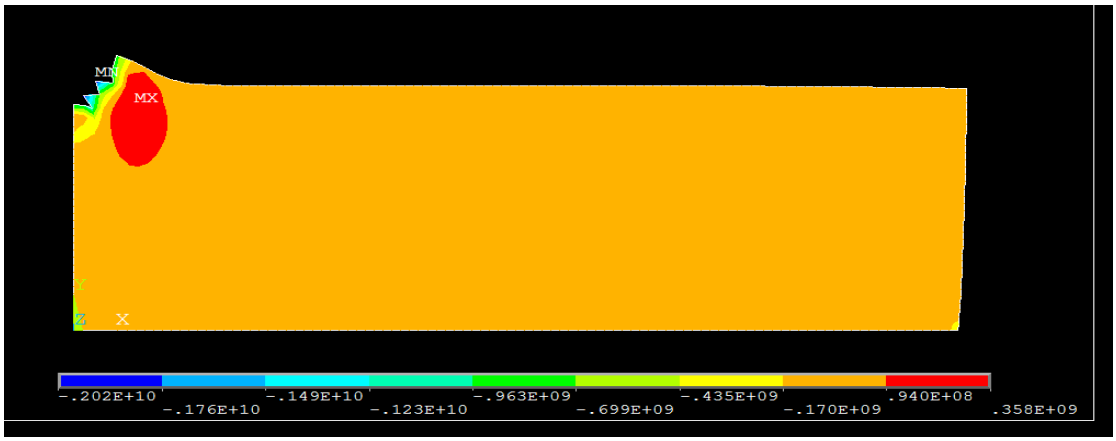

Fig.4 Residual Thermal stress in workpiece AISI 4340 in z-direction

5. RESULT AND DISCUSSION

This paper is focused on measuring the residual stresses in EDMed component using X-ray diffraction technique for the validation of the FEM results. The X-RAY DIFFRACTION (XRD) method of residual stress measurement that provides an accurate and well established result. The only crystals which diffract x-rays are those which are properly oriented relative to the x-ray beam to satisfy Bragg's Law,

$$n\lambda = 2d\ sin\theta \tag{8}$$

If we express the strain in terms of the crystal lattice spacing,

$$\varepsilon_{\emptyset} = \frac{d_{\emptyset} - d_o}{d_0} \tag{9}$$

Where, $d_{\emptyset}$ is the lattice spacing measured in the direction defined by $\emptyset$ and the d_o is the stress-free lattice spacing.

By finding the strain value of the material AISI 4340 from the above equation. we simply find out the value of the residual stresses in the workpiece. The stress equation is

$$\sigma = E\ \varepsilon_{\emptyset} \tag{10}$$

Here, σ is the residual stresses, E is the young's modulus of the material AISI 4340 i.e 200GPa. $\varepsilon_{\emptyset}$ is the strain defined in crystal lattice spacing.

By conducting the experiment of X-ray diffraction by X-ray diffractometers. We have validate the residual stresses solving by ANSYS and the experiment. The experiment was conducted on the Bruker D8 X-ray diffractometers, where Bruker D8 X-ray

diffractometers are designed to easily accommodate all X-ray diffraction applications in material research, powder diffraction and high resolution diffraction.

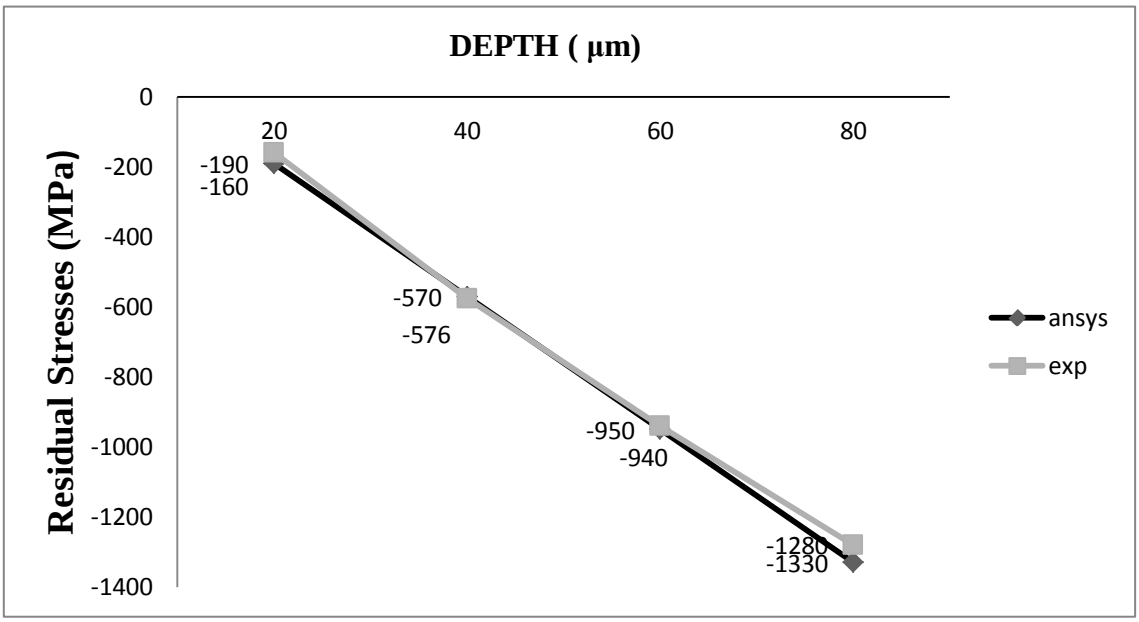

Fig.6.3 Comparison of residual thermal stresses (MPa) of Experimental Data and ANSYS Data

6. CONCLUSION

Result from the experimental and FEM thermal residual stresses have been presented during electric discharge process. From comparison the residual stresses of experimental and FEM result we find the compressive residual thermal stresses present in the workpiece.

REFERENCES

1) Vinod Yadav , Vijay K. Jain , Prakash M. Dixit, “Thermal stresses due to electrical discharge machining” International Journal of Machine Tools & Manufacture 42 (2002) 877–888 (2002)
2) J. Marafona*, J.A.G. Chousal, A finite element model of EDM based on the Joule effect. International Journal of Machine Tools & Manufacture 46 (2005) 595–602.
3) Nizar Ben Salah, Farhat Ghanem, Kaı¨s Ben Atig, Numerical study of thermal aspects of electric discharge machining process. International Journal of Machine Tools & Manufacture 46 (2006) 908–911.

4) Philip Allen, Xiaolin Chen, Process simulation of micro electro-discharge machining on molybdenum. Journal of Materials Processing Technology 186 (2007) 346–355.
5) H.K. Kansala, Sehijpal Singh, Pradeep Kumar, Numerical simulation of powder mixed electric discharge machining (PMEDM) using finite element method. Mathematical and Computer Modelling 47 (2008) 1217–1237.
6) Yeo, S.H., Kurnia, W., Tan, P.C. Critical assessment and numerical comparison of electro-thermal models in EDM. Journal of materials processing technology (2008); 203:241–251.
7) S.N. Joshi, S.S. Pande, Thermo-physical MODELLING of die- sinking EDM process. Journal of Manufacturing Processes 12 (2010) 455-463.